Compressed Core Characterization of a Cryogenic D_2 Target at Peak Neutron Production

Nicole Toscano

Compressed Core Characterization of a Cryogenic D_2 Target at Peak Neutron Production

Nicole C. Toscano
Greece Arcadia High School
Rochester, N.Y.

Advisor: Vladimir A. Smalyuk
Research Scientist

Laboratory for Laser Energetics
University of Rochester
Rochester, N.Y.

Nicole Toscano

Compressed Core Characterization of a Cryogenic D_2 Target at Peak Neutron Production

Abstract

The accurate characterization of compressed targets uniformly irradiated by laser beams is of highest importance for the success of inertial confinement fusion (ICF). Computer programs have been developed and used to make such a characterization based on a number of experimental measurements of the target core near peak compression. The temperature and density profiles of the hot compressed core of a cryogenic deuterium target have been characterized using measured fusion neutron yields, the neutron-averaged ion temperature, and the x-ray image at peak compression.

I. Introduction

The society in which we live is dependent upon natural resources for our survival as well as technical and intellectual progress. However, the consequences of burning fossil fuels such as natural gas, coal, and oil are devastating to the environment and humanity. The burning of these energy sources produces large amounts of carbon dioxide and sulfur. Nitrous oxides already present in the air combine with sulfur producing sulfuric acid and nitric acid forming acid rain. Acid rain damages trees and depletes the soil of nutrients, causing the soil to become more toxic. In industrialized nations such as the United States red spruce forests have become

more susceptible to damage as a result of acid rain. Acid rain also affects the pH of bodies of water, lowering their pH enough to alter the reproductive activities of certain fish species. Global warming, widely believed to be due to the presence of excessive amounts of carbon dioxide in the atmosphere is another prime example of how burning fossil fuels can impact the environment. Potentially the consequences of burning natural resources could dramatically change the climate of Earth if it is not stopped. Many are concerned with the amount of fossil fuels that are left for consumption. Oil is expected to run out in about 50 years at the current rate of consumption. As a result it is imperative for alternative energy sources to be produced in the near future.

To ensure the survival of humanity and the stability of the environment it is necessary for the scientists of today to develop an alternate means of energy production. For the past 50 years fission has been viewed as a promising method for producing energy. In fission nuclear reactions, high Z-elements split. As the atoms breakdown into less complex elements energy is released. However, this process produces highly radioactive materials which are harmful for both animal and plant life. As a result, many nuclear fission programs have been suspended internationally.

An alternative to this process is fusion. In fusion nuclear reactions, lighter elements are combined to form heavier ones with a release of energy. Fusion is a very promising source of energy as compared to fission and especially to the burning of fossil fuels. Neither the reactants nor the products in a fusion reaction are significantly radioactive, making fusion much safer for the environment. Additionally the resources are abundant. 1 km^3 of ocean water provides enough of the hydrogen isotope deuterium to replace the rest of the world's supply of oil which

amounts to roughly 500 billion barrels. Fusion already plays a vital role in life on Earth. The energy produced in the sun and the stars occurs as a result of fusion reactions.

As on the sun, hot and dense plasma needs to be produced in order for the fusion reactions to take place. In the sun fusion occurs at high temperatures ~10,000,000°K and high densities of $\sim 10^{25}$ electrons/cm^3. Therefore it is a challenge for scientists to create and control plasma at such critical conditions in the laboratory. There are different approaches to achieve this, including magnetic confinement fusion (MCF) and inertial confinement fusion (ICF). MCF uses a magnetic field to retain the plasma, allowing for the nuclear reactions to take place. In ICF, lasers and charged particle beams are used to create high temperatures and densities within the central parts of the pellet (target core) creating nuclear reactions. In direct-drive ICF, a large number of laser beams are focused uniformly on the target to achieve uniform compression and heating.[1]

Laser-driven ICF is a three step process and can be seen in Fig.1. The pellet containing fusion fuel, typically the hydrogen isotopes of deuterium and tritium, is first irradiated using laser energy. A large number of beams is necessary for uniform irradiation [see Fig.1 (a)]. The target reaches an extreme temperature causing the outer portion to expand and blowoff. As a result of Newton's Third Law the pellet then implodes, compressing the fuel within it [see Fig.1 (b)]. At peak compression, when high temperatures and densities are achieved in the target core, the deuterium (D) and tritium (T) of the fuel are able to react releasing neutrons and charged particles as shown in Fig. 1(c). A large amount of energy is released in each fusion reaction. Currently, ICF is a leading area of research in scientific laboratories throughout the world.[2]

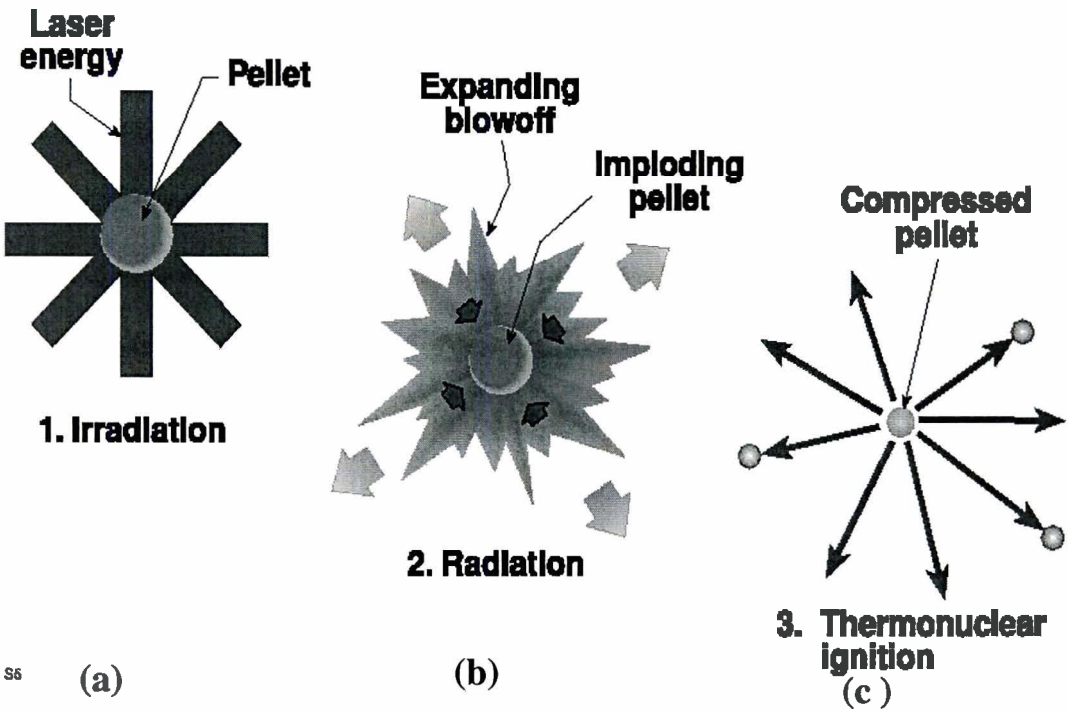

Figure 1: Schematic of the target implosion in laser driven ICF.
(a) Irradiation. Many laser beams directly illuminate the target for uniform compression.
(b) Radiation. While the outer part of the target is ablated the inner part moves to the center.
(c) At peak compression fusion reactions occur in high temperature and high density plasma.

The Laboratory for Laser Energetics (LLE), in Rochester, NY currently possesses the most powerful laser system (the OMEGA laser) in the world, used for ICF research. The OMEGA laser, which is the size of a football field, has 60 beams allowing for a uniform heating of small, ~1mm diameter targets. The more laser beams there are the more the more uniform the target is heated. One of the goals of ICF research and of the OMEGA laser[3] program in particular is to study, approach, and achieve ignition using cryogenic DT and D_2 capsules.

Scientists have not yet met this goal but they are on their way to achieving it.

In order for ignition to occur the energy that is produced from fusion must be equivalent to or greater than the laser energy that is input into the system. The most energetically favorable fusion reaction for energy production is $D+T \rightarrow He^4(3.5MeV)+n(14.1MeV)$. Each reaction releases 2.8 x 10^{-12} J of energy (or 17.6 MeV). In the case of the OMEGA laser, 30 kJ of energy is input into the target through the 60 beams in laser light; therefore, to ignite the target, it is necessary to achieve a total yield of ~1.0 x 10^{16} fusion reactions in one implosion. The target on OMEGA is 1 mm in diameter containing ~100 μm thick deuterium-tritium (DT) ice.[4] The ice is created at a cryogenic temperature of ~18°K.

While DT fuel will be used primarily for energy production, targets with cryogenic D_2 fuel are very helpful for hot core characterization at peak compression. Ion temperature, areal density, and convergence ratio are more easily measured in D_2 fuel than in DT fuel.[5] There are two primary fusion reactions in D_2 fuel:

1a. $D+D \rightarrow T(1.01MeV)+p(3.02MeV)$

1b. $D+D \rightarrow {}^3He(0.82MeV)+n(2.45MeV)$.

Each of these reactions has a 50% chance of occurring. The first primary reaction produces a triton, T, which can react with a deuteron, D, through the secondary reaction

2. $D+T(0-1.01MeV) \rightarrow {}^4He+n(11.9-17.2MeV)$.

The yields of both DD primary and DT secondary reactions depend on the temperature and density of the compressed core.

One of the most critical aspects of the ICF program is a characterization of the fuel during peak compression. It is necessary to access the efficiency of implosion and to guide

future experiments. Such comprehensive characterization is very challenging because the implosion happens during a very short period of time (~1 ns) and the size of the fuel core at peak compression is very small, about ~100 μm. The primary goal of this project was to find out if the experimental observations such as neutron yields of fusion reactions, core x-ray images could provide comprehensive information about the structure (temperature and density distribution) of the hot core at peak compression. It was found that the temperature and density profiles can be inferred from the measured primary DD and secondary DT neutron yield, the measured neutron-averaged ion temperature, and the measured x-ray images of core emission, as presented in this article. These profiles will be used to optimize the target designs of the ignition experiments planned in the near future.

During the target implosion, any perturbations present grow due to Rayleigh-Taylor (RT) instability[6], compromising target performance and reducing fusion yield. To overcome this obstacle, more stable target designs are proposed which include using bigger, more massive targets driven with more powerful laser systems. The effect of detrimental perturbation growth due to RT instability is much less in bigger targets.[5] To support the goal of ignition and high gain, the National Ignition Facility (NIF) is currently being built in Livermore, California. This 1.8 MJ, 192 beam laser system is expected to ignite cryogenic DT targets. To achieve ignition on NIF, the experiments on OMEGA study physics of various aspects of ICF. The project that I was involved, presented in this article, is directly related to the most important physics aspect of ICF – characterization of the hot core at peak compression of spherical implosion.[7]

II. Experimental Conditions

The schematic for the cryogenic capsule used in shot 28900 is shown in Fig. 2. The 1-mm diameter target has a shell with an outer ~5-μm-thick CD layer and an inner layer of ~100 μm thick D_2 ice, made at a temperature of ~18 K. The target was driven with a 23-kJ, 1-ns pulse by the 60-beam OMEGA laser system containing ~23 kJ of on-target energy. The laser beams were smoothed using a series of two processes including spectral dispersion (2-D SSD)[8] and polarization smoothing (PS)[9]. The primary DD neutron yield was 1.24 x 10^{11} ± 7.64 x 10^{8} with a neutron-averaged ion temperature (measured with neutron time of flight) of 3.6 ± 0.5 keV and the measured neutron burn width was ~170 ± 25 ps. The secondary DT yield was 1.17 x 10^{9} ± 3.17 x 10^{7}. Images of the target at peak neutron production were measured using an x-ray framing camera. The camera has a spatial resolution of ~10 μm, a temporal resolution of ~40 ps. The temperature and density profiles of the target core at peak compression can be inferred using these experimentally measured values and time-resolved target x-ray images.

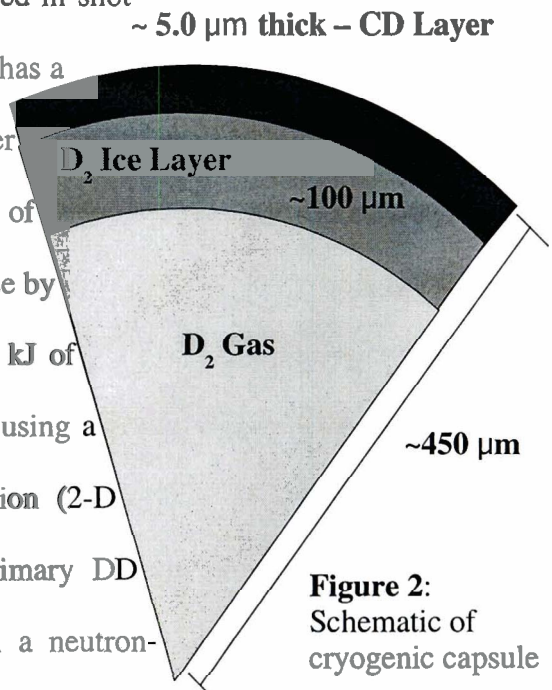

Figure 2: Schematic of cryogenic capsule

III. Program Description

Since neutron yields and core x-ray images depend on temperature and density profiles inside the core, the goal of this project was to determine these profiles from the measured neutron and x-ray emissions. Modeling of the target was based on computer programs which varied core temperature and density profiles and then calculated neutron yields, neutron-averaged ion temperature, and x-ray images. Only those profiles which generated neutron and x-ray data consistent with experimentally measured observations were chosen.[7]

The program was set up into four stages. The first stage produced a series of temperature and density profiles that were consistent with the primary DD neutron yield and neutron-averaged ion temperature. Results from this stage were carried over into stage two. Profiles that matched the secondary DT neutron yield were chosen for further analysis. Similar calculations were carried out for a number of core electron pressures ranging from 1 to 10 Gbar in the third stage. Finally the temperature and density profiles consistent with the measured core x-ray image were chosen in the fourth stage of modeling. A series of assumptions were made when modeling the core. First it was assumed that the core of the target was made completely of ionized deuterium ideal gas and that the pressure within the core remained constant. Temperature and density profiles produced were based on a spherically-symmetric target. The core was assumed to be not evolving during peak neutron production.

Figure 3(a) shows two possible temperatures profiles out of about 10^{10} considered in the first stage modeling. Only monotonically decreasing temperature profiles were considered for analysis. The grid used in this modeling had distance increments of 20 μm and temperature increments of 250 eV. Additional grids were produced for distance steps of 15, 10, and 5 μm.

More detailed grids were used for calculations at higher electron pressures. These more specific grids increased the time it took for the program to analyze the ~10^{10} temperatures profiles. It was determined that for higher resolutions the program would run for days and sometimes even years before it had completed its necessary task. So we spent a lot of time looking for computation conditions which produced accurate results during a reasonable period of time. Most major physical processes were already incorporated into the programs. These processes included 1) charge particle propagation in plasmas (for triton slowing down and the secondary DT yield calculations), 2) radiation transport of x-rays in plasma, 3) primary DD yield calculations for every particular temperature-density profile, 4) x-ray image construction. In order to perform calculations in a reasonable time, a lot of programming and optimization was performed to optimize calculations, which vary different parameters to understand the sensitivity of results from various physical parameters.

Corresponding density profiles were produced using an ideal gas relationship between temperature $T(\mathbf{r})$ and density $n(\mathbf{r})$. For any given temperature profile the corresponding density profile was determined using this ideal gas equation, $P_e(\mathbf{r})=n(\mathbf{r})T(\mathbf{r})$. The results of stage 1 calculations for a particular electron pressure of 2.6 Gbar are shown in the gray

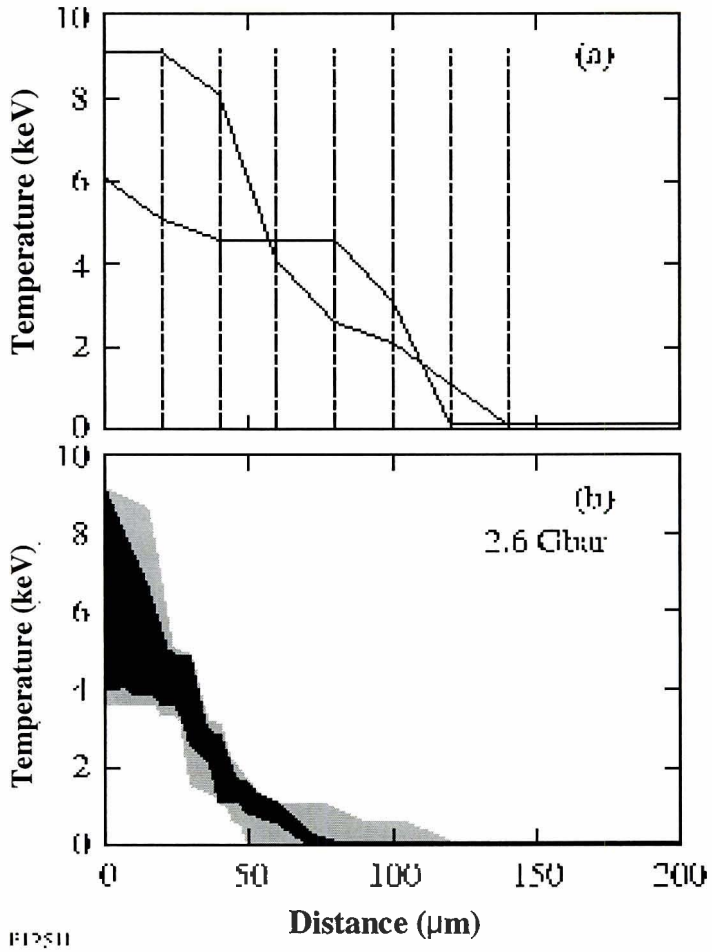

Figure 3: (a) The temperature grid with 250 eV temperature steps and a distance step of 20 μm as shown by the dots. The two lines represent monotonically decreasing temperature profiles produced as a function of distance and were used in core modeling.
(b) Temperature profiles in the light-shaded region that satisfy primary DD yield and neutron-averaged ion temperature and in addition secondary DT yield in the dark-shaded region are calculated at an electron pressure of 2.6 Gbar.

region of Fig. 3(b). This corresponds to temperature profiles that are consistent with the

measured DD neutron yield and neutron-averaged ion temperature. These profiles were passed on to the second stage, which eliminated all profiles inconsistent with the measured DT neutron yields. The black region in Fig. 3(b) indicates the results of the second stage calculations. These profiles are consistent with all neutron measurements, i.e. DD and DT neutron yields and the neutron-averaged ion temperature.

In the third stage of modeling similar profiles (as shown in Fig. 3) were constructed at different electron pressures ranging between 1 and 10 Gbar. It was found that only at pressures above 1.3 Gbar there are solutions which can produce the desired yields and ion temperatures. Examples of these solutions for particular pressures of 1.3, 2.6, 5.1 Gbar are shown in Fig. 4(a). It was found that the sizes of x-ray images are different for different pressures and therefore can be used to finally determine the temperature-density profiles consistent with all neutron and x-ray measurements.

The fourth stage of modeling was to compare calculated sizes of x-ray emission for different electron pressures and compare those with the experimentally measured core size. This is necessary to finally determine temperature and density profiles consistent with experimental x-ray images. Since it takes a significant amount of time to calculate the x-ray image from the given temperature and density profiles, only one representative x-ray image was calculated for each particular electron pressure. The examples of radial lineouts calculated for electron pressure 1.3, 2.6, and 5.2 Gbar [the same pressures shown in Fig. 4(a)] are shown in Fig. 4(b). The size of x-ray image is very sensitive to electron pressure. At a higher pressure the core size is smaller. The radii produced for 1.3, 2.6, and 5.1 Gbar were 130, 80, and 40 μm, respectively. This enabled us to narrow down the large range of temperature and density profiles (consistent

with neutron data) to a relatively narrow range consistent also with measured x-ray image.

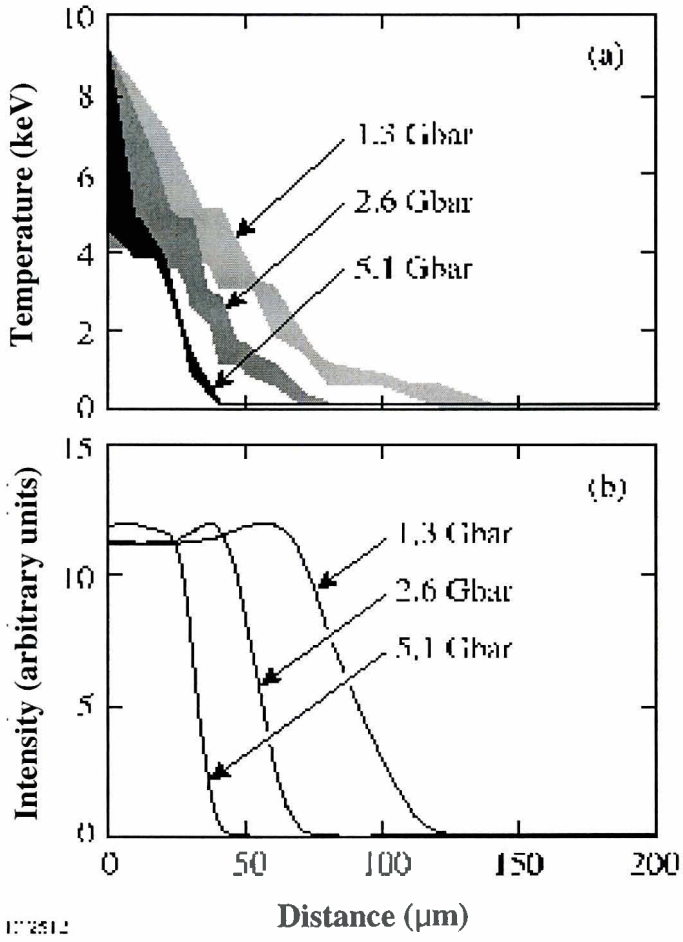

Figure 4: (a) Temperature profiles that match primary DD, secondary DT yields, and measured average-ion temperature at 1.3 (light), 2.6 (medium), and 5.1 Gbar (dark).
(b) Examples of radial lineouts calculated for electron pressures of 1.3, 2.6 5.2 Gbar.

Figure 5(a) shows the image of the target in the shot 28900 at peak neutron production.

This image also shows lineouts through the center in two perpendicular directions.

Calculated radial lineouts that are most similar to the experimental ones are represented by the shaded region which corresponds to a range of electron pressures between 2.3 and 3.1 Gbar. Finally, the temperature and density profiles that most accurately correspond to the primary DD yield, the secondary DT yield, the neutron-averaged ion temperature, and the x-ray images can be seen in Fig. 5(b). Profiles in the light shaded region are the temperature profiles while those in the dark are the density profiles. As can be seen in Fig. 5(b), only a narrow range of the billions of temperature and density profiles that were originally generated by the computer program remained consistent with all neutron and x-ray measurements.

IV. Conclusion

For the first time, the density and temperature profiles of the compressed core of a cryogenic target at peak neutron production have been characterized. The core pressure was inferred to be between 2.3 and 3.1 Gbar based on experimentally measured primary DD and secondary DT yields, the average ion temperature, and core x-ray images. It is very important to understand these temperature and density profiles and their variations on neutron production. By measuring details of the core structure at peak neutron production scientists can adjust their target designs to achieve ignition in future experiments.

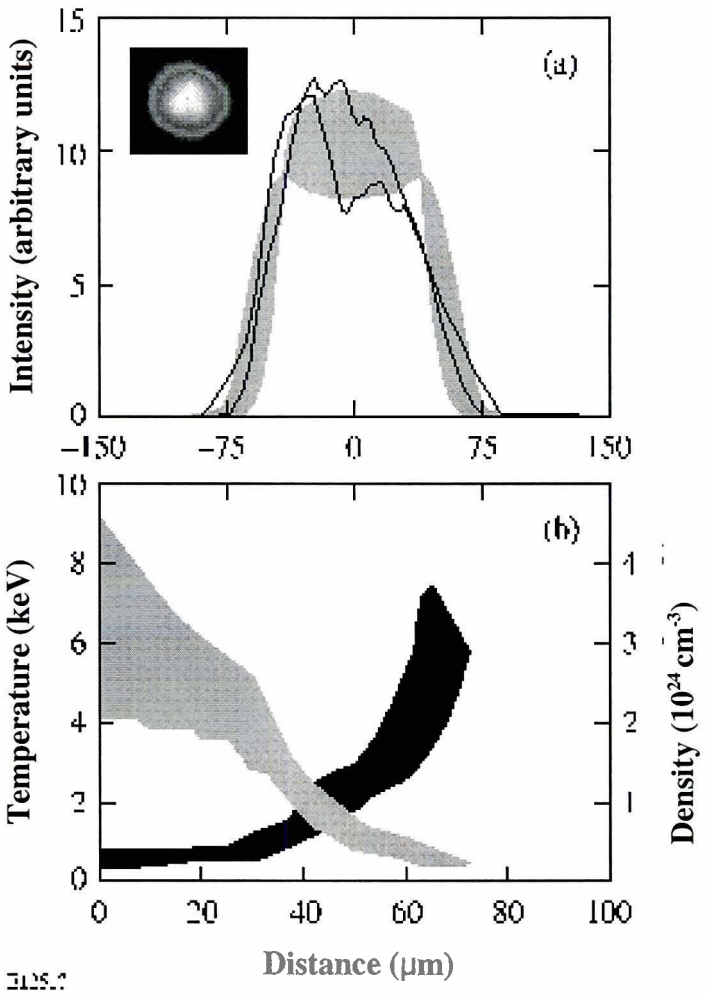

Figure 5: (a) The measured image of the target core at peak neutron production by the x-ray framing camera can be seen in the upper left quadrant. Thick and thin lines represent the horizontal and vertical radial lineouts of the experimental data while the shaded region corresponds to lineouts calculated at electron pressures of 2.3 and 3.1 Gbar. All lineouts were normalized to the same area under the curve.

(b) Core temperature (light-shaded) and density (dark-shaded) profiles that correspond to electron pressures from 2.3 to 3.1 Gbar that are consistent with the x-ray emission of the core image.

VI. Acknowledgments

Most importantly I would like to recognize my advisor Vladimir A. Smalyuk for his guidance and patience throughout this summer. His countless hours of assistance were greatly appreciated and allowed me to successfully complete my project and grow in a knowledgeable environment. Greatly appreciated was the assistance Sonya B. Dumanis gave to me on a daily basis. I would also like to show my appreciation to those who assisted me in completing my project including J. Delettrez, R. Epstein, V. Glebov, B. Radha, and C. Stoeckl. I would also like to thank Dr. Stephen Craxton for allowing me to participate in the Summer Research Program at the Laboratory for Laser Energetics and for reviewing this manuscript. Thank you.

VII. References

[1]S. E. Bodner, D. G. Colombant, J. H. Gardner, R. H. Lehmberg, S. P. Obenschain, L. Phillips, A. J. Schmitt, J. D. Sethian, R. L. McCrory, W. Sekra, C. P. Verdon, J. P. Knauer, B. B. Afeyan, and H. T. Powell, Phys. Plasmas **5**, 1901 (1998).
[2]J. D. Lindl, *Inertial Confinement Fusion: The Quest for Ignition and Energy Gain Using Indirect Drive* (Springster, New York, 1998).

[3]T. R. Boehly, D. L. Brown, R. S. Craxton, R. L. Keck, J. P. Knauer, J. H. Kelly, T. J. Kessler, S. A. Kumpan, S. J. Loucks, S. A. Letzring, F.J. Marshall, R. L. McCrory, S. F. B. Morse, W. Seka, J. M. Soures, and C. P. Verdon, Opt. Commun. **133**, 495 (1997).

[4]T. C. Sangster, J.A. Delettrez, R. Epstein, V. Yu. Glebov, V. N. Goncharov, D. R. Harding, J. P. Knauer, R. L. Keck, J. D. Kilkenny, S. J. Loucks, L. D. Lund, R. L. McCrory, P. W. McKethy, F. J. Marshall, D. D. Meyerhofer, S. F. B. Morse, S. P. Regan, P. B. Radha, S. Roberts, W. Seka, S. Skupsky, V. A. Smalyuk, C. Sorce, J. M. Soures, C. Stoeckl, and K. Thorp, Phys. Plasmas **10**, 1937 (2003).

[5]P. W. McKentry, V. N. Goncharov, R. P. J. Town, S. Skupsky, R. Betti, and R. L. McCrory, Phys. Plasmas **8**, 2315 (2001).

[6]V. A. Smalyuk, J. A. Delettrez, V. N. Goncharov, F. J. Marshall, D. D. Meyerhofer, S. P. Regan, R. C. Sangster, R. P. J. Town, and B. Yaakobi, Phys. Plasmas **9**, 2738 (2002).

[7]V. A. Smalyuk, J.A. Delettrez, S.B. Dumanis, R. Epstein, V. Yu. Glebov, P. W. McKenty, D. D. Meyerhofer, P. B. Radha, T. C. Sangster, C. Stoeckl, N. C. Toscano, J. A. Frenjie, C. K. Li, R. D. Petrasso, F. H. Seguin, and J. A. Koch, *"Hot-Core Characterization of the Cryogenic D_2 Targets at Peak Neutron Production in Direct-Drive Spherical Implosion"*, submitted to Phys. Rev. Lett. (2003).

[8]S.P. Regan, J. A. Marozas, J. H. Kelly, T. R. Boethly, W. R. Donaldson, R. A. Jaanimagi, R. L. Keck, R. J. Kessler, D. D. Meyerhofer, W. Seka, S. Skupsky, and V. A. Smalyuk, J. Opt. Soc. Am. B **17**, 1483 (2000).

[9]T.R. Boehly, V. A. Smalyuk, D. D. Meyerhofer, J. P. Knauer, D. K. Bradley, R. S. Craxton, M. J. Guardalben, S. Skupsky, and T. J. Kessler, J. Appl. Phys. Plasmas **85**, 3444 (1999).